# Experiment 6 and 7: Physical Pendulum Harmonic Oscillations and Waves on Vibrating String

Kubilay Agi

UID: 304784519

Lab Date: 29 August, 5 September 2018

Lab Section 8 – Monday/Wednesday 11:30am

TA: Jordan Runco

Partner: Shannon Largman

Abstract Word Count: 197

**Abstract**

**Harmonic Oscillations in Pendulums and Strings**

[1]K. Y. Agi

Our experiment investigates the nature of harmonic oscillations in two different systems: a physical pendulum and tensioned string. The pendulum swung freely in the undamped, undriven trials, and it swung through magnets for the damped cases. We determined that the oscillation resonance frequency was (0.711 ± 0.001) Hz in the undamped cases and (0.657 ± 0.005) in the damped cases. We identified the magnet separation distances for each of the three regimes of damping. We found that (13.0 ± 0.5) mm was the separation that produces critical damping. Larger gaps produce an underdamped oscillating system, and smaller gaps produce an overdamped system. We also used various methods to determine the quality-factor of the system to see how underdamped the system is. We determine which method produced the most accurate result for our experiment. For the vibrating spring, we sent waves through a tensioned string with a wave driver. We first determined the wave speed for each value of applied tension. Then we found the frequency for the first through ninth harmonic of the string. Finally, we pinched the string in the middle and found that even harmonics are unaffected by the restriction, but odd harmonics are affected.

[1]Department of Engineering and Applied Science, University of California, Los Angeles.

## Introduction

These experiments aim to observe the properties of harmonic motion in physical pendulums and vibrating strings. These physically different systems both exhibit characteristics of harmonic motion. The two systems oscillate in different ways, but each system allows us to explore different aspects of harmonic motion more easily than if we used the other one.

With the pendulum, we seek to verify that the resonance frequency of the undamped, undriven oscillations is the same as the resonance frequency of damped, driven oscillations. In this experiment, we swing the metal pendulum through a pair of magnets with variable separation. This allowed us to identify the magnet separation distances at which the oscillating system undergoes critical damping, overdamping, and underdamping. Additionally, we used damped oscillations to calculate the quality factor of the system.

The vibrating string experiment provides insights into the harmonics in an oscillating system. With the wave driver, we produced pulses that sent waves traveling back and forth through the string. We found the relationships between applied tension, linear mass density, and wave speed. We also found the frequencies at which the string vibrated at its $n^{th}$ harmonic. Finally, we looked at how restricting the vibrating string at its middle point affects even and odd harmonics.

## Methods

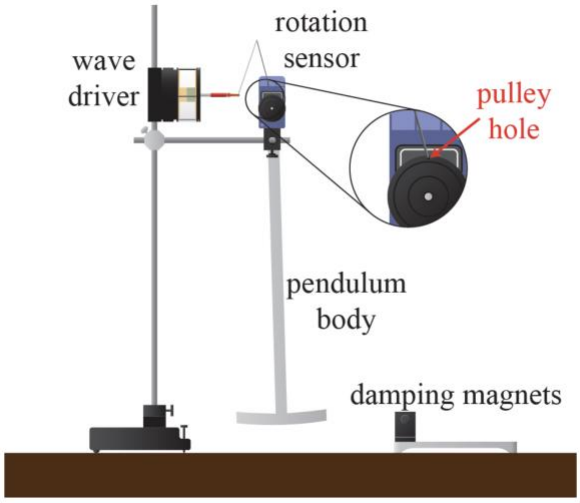


**Figure 1, Physical Pendulum Experiment Apparatus[1]:** This image shows the setup of the equipment that was used for the experiment involving a physical pendulum. For the first part of that experiment, the wave driver was off and disconnected from the rotation sensor. In the second part of the pendulum experiment, the wave driver was used to produce waves in the pendulum. We also included a photogate to record the period of the oscillations, but this is not illustrated in the image.

*Pendulum Experiment Method*

In the first part of this experiment, we look at undriven oscillations. We define the equilibrium point as the point where the pendulum is at rest, pointing vertically downward. We also designated the direction toward the vertical rod as the positive direction and the direction toward the damping magnets as the negative direction. We set our data acquisition system (DAQ) to record the angle from equilibrium in time steps of 0.04 seconds (25 Hz).

For the undamped trial, we move the magnets away from the apparatus to avoid any unintended damping on the system. We placed our photogate next to the vertical rod. We started the edge of the pendulum at the point where it begins to block the photogate sensor. We do this so that we can have a consistent starting point, and also so that we can record the period of the pendulum as it swings. To measure oscillation period, we set up our DAQ so that it records times starting when the photogates goes from blocked to unblocked and finishes timing the oscillation when it goes from unblocked to blocked. Then we release the pendulum and let it swing for a few seconds, so we can record enough data.

For the damped trial, we place the magnets at the equilibrium point so that the point where the vertical bar of the pendulum connects with the horizonal bar sits within the two magnets. To identify the magnet separation at which critical damping occurs, we decrease the separation for every trial, until we reached overdamping. We start at a (50.0 ± 0.5) mm of separation and decrease the distance by about 10 – 12 mm for each trial. We kept the photogate in the same place so that we have a consistent starting point for each trial.

Next, we look at driven oscillations. For this part of the experiment, we hook up the wave driver to the rotation sensor. We leave the magnet in the same place as they were for the damped undriven oscillation trials (at the equilibrium point). We used a magnet separation of (26.5 ± 0.5) mm for this trial. We use 4 V as our voltage. We turn on the wave driver and determine the resonance frequency by analyzing the Lissajous graphs. We find the frequency at which the Lissajous plot was horizontal without any tilt. It is useful to find a range of values where it is not possible to find differences between the plots. This provides the uncertainty for the measurement.

Also, to determine the amplitude response to frequency of oscillation, we recorded the amplitudes of oscillation for 13 different frequencies. These data points provide us with another method to calculate the Q-factor.


**Figure 2, Vibrating String Experiment Setup**[1]**:** This image shows the setup for the vibrating string experiment. Though it is not shown in this image, we had extra vertical rods on the hanging mass side to support the laser and the photodiode.

*String Experiment Method*

For this experiment, we use a wave driver to generate waves on a string. We tie a knot in the end of the string to hook the masses onto it. We make sure to measure the length of the string used to tie the knot because this length will be subtracted off of the length of the stretched string. We needed to measure the parts of the string in increments because the meter ruler was not long enough to cover the entire string. It helped to have a marker with us, so we could keep track of where the next measurement should start from. The string is stretched out by running the string over a pulley and hanging a mass off of the end. This is shown in Figure 2.

In addition to measuring the length of the string, we also make a note of the string's mass. This value is needed to determine the linear mass density. After we record the mass of the string, we also record the masses of each mass that we will hang from the string. We use a balance scale to measure the mass of each object. The scale only measures up to 110 g, so we need to use some masses as a counterweight to record the mass of the heavier objects.

We point a laser horizontal to the table so that the laser's light covers the upper third of the string. A photodiode is pointed downward at the string so that its sensor is directly above the portion of the string that the laser is on. The intensity of the laser's light on the string differs when the string oscillates. Light intensity is the value that we set the data acquisition system (DAQ) to record against time. We also have the DAQ record the output voltage that is sent to the wave driver so that we can see when the waves are generated.

The first sets of data do not involve the wave driver. We hang the 100 g, 200 g, and 350 g mass onto the end of the string hanging over the pulley. We measure each segment of the stretched string for each mass separately with our meter ruler. We measure from the clamp by the wave driver to the pulley, and then from the pulley to the start of the knot. We also measure the diameter of the pulley so that we can calculate the length of string that is on the pulley. The sum of these lengths is the stretched length in part one of the experiment. With this data for each mass, we can calculate the linear mass density and applied tension. Then, we can

determine the predicted wave speed for when each mass is attached. After taking our measurements, we turn the wave driver on at 0.5 Hz and record several seconds of data for each mass that is attached. We record the timestamps in seconds, light intensity as a percentage, and output voltage in volts. With the data that we record, we look at the peaks of the graph of light intensity versus time, and we find the time differences between each consecutive peak to determine the time that it took each wave to travel along the string.

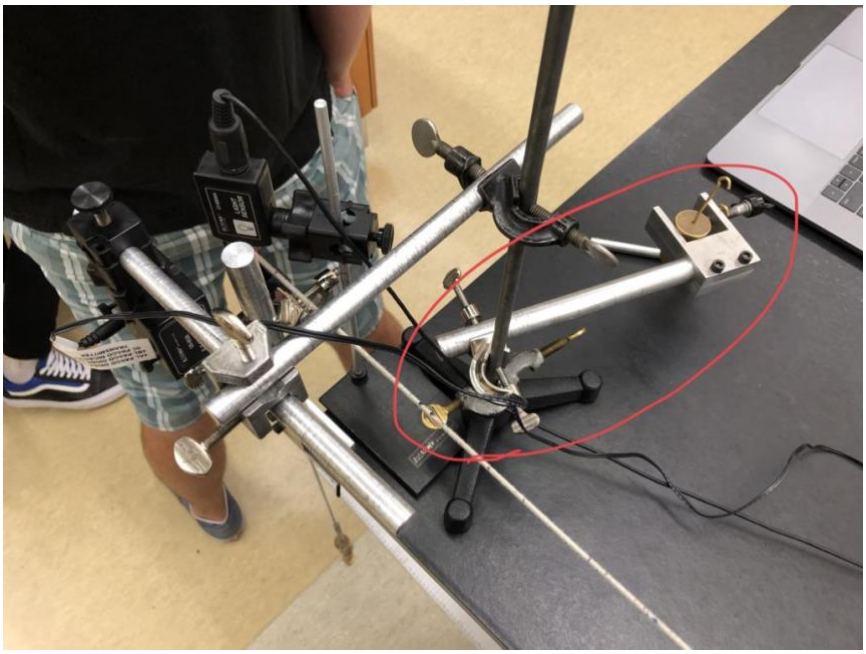

**Figure 3, Counterbalance for Part Two of String Experiment:** This is an image I took of the counterbalance we used to prevent the vertical rod from tipping over. The laser was attached to this rod, and this made it too top heavy. We used an extra rod and masses as the counter balance (circled in red).

After these recordings, we leave the 350 g mass hanging on the end of the string. We move the laser and photodiode to about one centimeter from the apex of the pulley. This is close to the node of the oscillating string. We need to move it closer to the node so that the amplitude of oscillation is lower, and the laser can remain on the string. Our apparatus to suspend the laser tended to tip over because it was too top heavy. We fixed this issue by adding a counter balance to the apparatus (shown in Figure 3). We now find the fundamental frequency of the string by looking at the parametric Lissajous plots produced by the DAQ by plotting light intensity versus wave driver frequency. From here, we predict the frequencies for each harmonic. We use these estimations as a starting point when looking at the Lissajous plots and adjusted them to find the actual value according to the results from the DAQ.

Finally, we pinched the string with our fingers halfway between the clamp and the pulley. Ideally, we would use a ring here to avoid introducing extra error into the experiment. We run the wave driver at the frequencies that produce the second, fourth, and fifth harmonic. The 350 g mass is still attached to the string for these trials. We keep our finger pinched in the same

place for all three trials. We record the times and light intensities for the trials where the string was pinched in the middle. However, we ran out of time, so we were unable to record data for these harmonics when the string was not pinched.

**Analysis**

*Physical Pendulum*

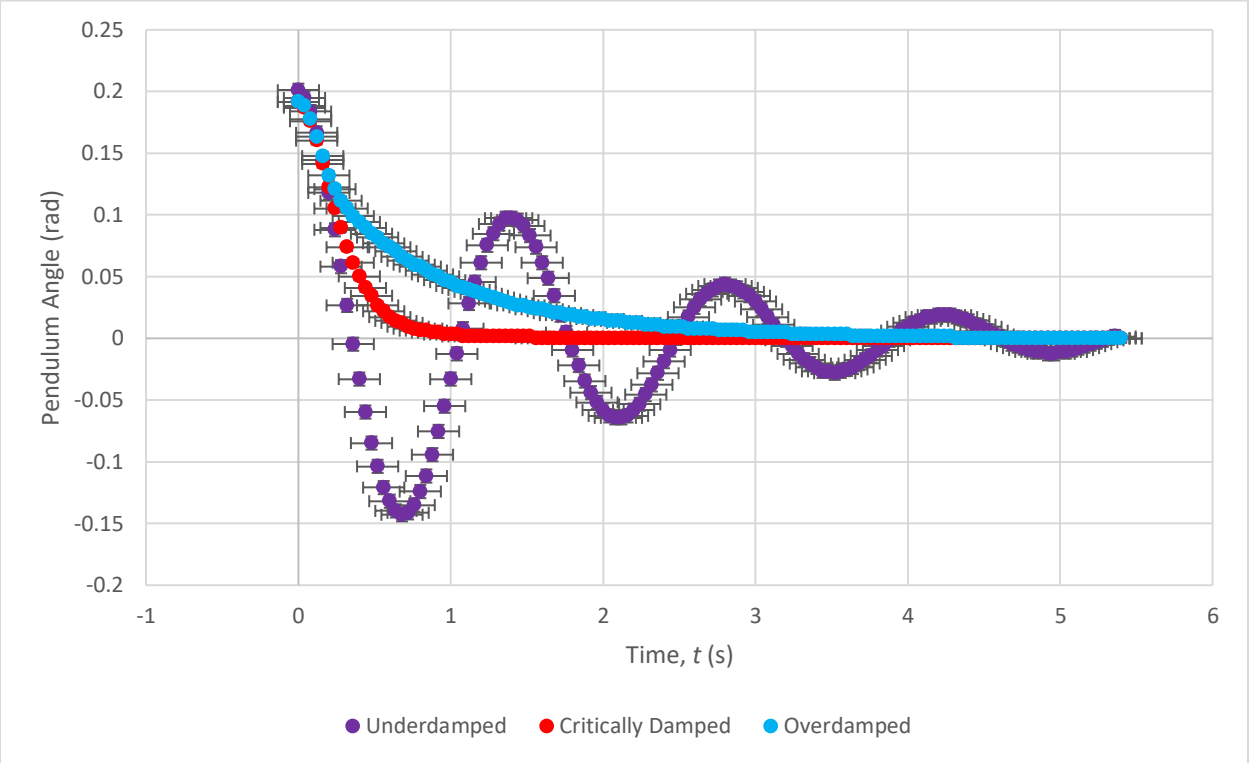


**Figure 4, Regimes of Damping with Different Magnet Separations:** This plot shows the angle of displacement of the pendulum from equilibrium during trials damped with magnets. The underdamped data points were produced using a magnet separation of (28.5 ± 0.5) mm. The overdamped oscillation was generated with a magnet separation of (7.5 ± 0.5) mm. The critically damped oscillation used a magnet separation of (13.0 ± 0.5) mm.

*Regimes of Damping*

Before the experiment, we hypothesized that larger gaps would result in underdamping and smaller gaps would produce overdamped results. We also expect to see that somewhere in between is the magnet separation distance where the system is critically damped. Our results confirm our hypothesis. (28.5 ± 0.5) mm was the larger gap and yielded underdamping, and (7.5 ± 0.5) mm was the smaller gap which yielded overdamping. Finally, (13.0 ± 0.5) mm is the separation that we found produces critical damping.

*Resonance*

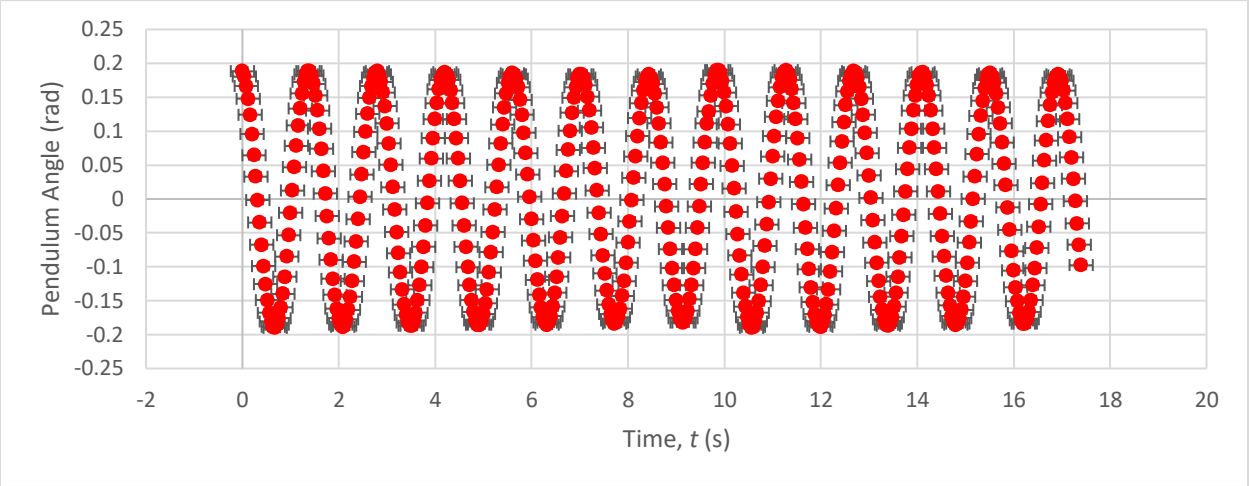


**Figure 5, Undamped Undriven Pendulum Oscillation:** This plot shows the data points that were recorded for the undamped, undriven oscillation. The data shows a simple harmonic oscillation of the pendulum. There is negligible decrease in the amplitude of oscillation over the course of the trial.

By looking at Figure 5 above, we see that for each *n* maxima, there are *n* – 1 cycles between each pair of adjacent extremum. To find the angular frequency of oscillation, we need to divide the number of cycles that occur within a certain time range by that time range.

$$\omega_0 = \frac{n-1}{t_n - t_1}$$

To find the uncertainty, we take the standard deviation $\sigma$ of the time differences between each adjacent pair of maxima. Then, we divide by the square root of the number of data points *n* that we used. In our case, *n* is 7 and $\sigma$ is 0.002 radians.

$$\partial\omega_0 = \frac{\sigma}{\sqrt{n}}$$

With these equations, we find that the angular frequency of oscillation for the pendulum in the undamped, undriven trial is (0.711 ± 0.001) Hz.

*Quality Factor*

This is the first method we will use to determine the quality factor of the oscillating pendulum. The quality factor (Q-factor) in an oscillation describes how damped an oscillator is. Oscillators with low quality factors have resonant frequencies in undriven, undamped cases that are significantly different than the resonant frequency during driven, damped oscillation.[1] Higher quality factors mean less difference between these two measured angular frequencies. [1]

To calculate the Q-factor for our oscillator with this method, we need to know the angular frequency during the damped, driven oscillation trial, and we need to know the damping time. The damping time is the time it takes the amplitude to decrease by a factor of $1/e$. We measured the resonance frequency of driven, damped oscillations to be (0.657 ± 0.005) Hz at a voltage of 4 V and a magnet width of (26.5 ± 0.5) mm. We used plots of Lissajous to determine the value of resonance frequency. The range in which we could not discern each plot from the others was 0.652 – 0.662 Hz, hence we have an uncertainty of ± 0.005. We can solve Equation 6.12[1] for the damping time $\tau$.

$$\omega_R = \sqrt{{\omega_0}^2 - \frac{2}{\tau^2}}$$

$$\tau = \sqrt{\frac{2}{{\omega_0}^2 - {\omega_R}^2}} = 5.20\ seconds$$

$$\partial\tau = \tau_{best}\sqrt{\left(\frac{\partial\omega_R}{\omega_R}\right)^2 + \left(\frac{\partial\omega_0}{\omega_0}\right)^2} = 0.04\ seconds$$

Now we can find the Q-factor for this experiment.[1]

$$Q = \frac{1}{2}\tau\omega_R = 1.71$$

$$\partial Q = Q_{best}\sqrt{\left(\frac{\partial\omega_R}{\omega_R}\right)^2 + \left(\frac{\partial\tau}{\tau}\right)^2} = 0.02$$

Our Q-factor is (1.71 ± 0.02). Q-factor is a dimensionless value and thus has no units. Our Q-factor here is relatively low. Our two values for damped angular frequency are (0.711 ± 0.001) Hz and (0.657 ± 0.005) Hz. These two values fall out of each other's error windows and their difference is statistically significant. We would expect that our values of angular frequency for undamped, undriven oscillation would match that of driven, damped oscillations.

It is possible that the resonance frequencies are different because of the difference in the swing amplitude between each trial. The angular displacement from equilibrium was much larger in the undriven, undamped case than in the driven, damped case.

*Q-factor via Ratio of Angular Frequencies*

We can also the find the Q-factor by looking at the ratio of resonance frequencies from the damped and undamped oscillations. This is our second method to determine the Q-factor. The ratio of the damped, driven resonance frequency to the undamped, undriven resonance frequency is[1]:

$$\frac{\omega_R}{\omega_0} = \frac{1}{\sqrt{1 + \frac{1}{2Q^2}}}$$

Solving for Q, we get the following equation:

$$Q = \sqrt{\frac{1}{2\left[\left(\frac{\omega_0}{\omega_R}\right)^2 - 1\right]}} = 1.71$$

Plugging in our values for $\omega_0$ and $\omega_R$, our value for the Q-factor is (1.71 ± 0.01). This result agrees with our Q-factor from the previous method. The uncertainty for this Q-factor was determined through the propagation of uncertainties with $\omega_0$ and $\omega_R$, which are the only two values with uncertainty in the equation.

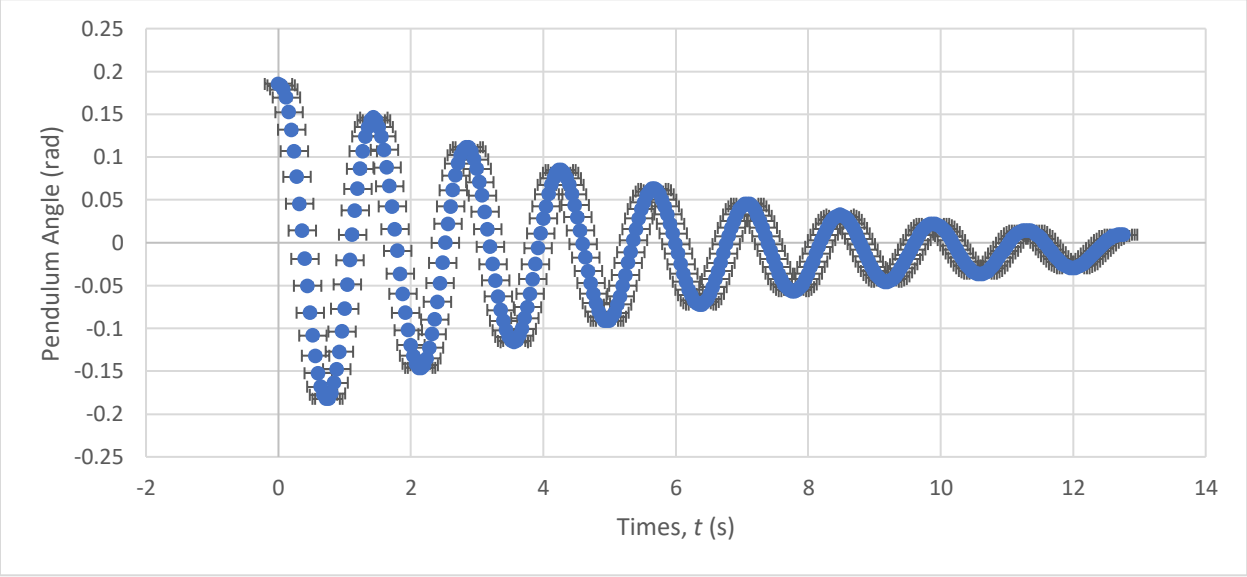


**Figure 6, Damped Undriven Pendulum Oscillation:** This plot shows how the angle of the pendulum (in radians) from equilibrium changes as time goes on. The amplitude of oscillation decreases because of the damping from the magnets. Eventually, the data points should converge to 0. However, they appear to be a bit offset here. This is likely because the magnets were not precisely at the equilibrium point of the pendulum. The magnet separation in this damped trial was (38.0 ± 0.5) mm.

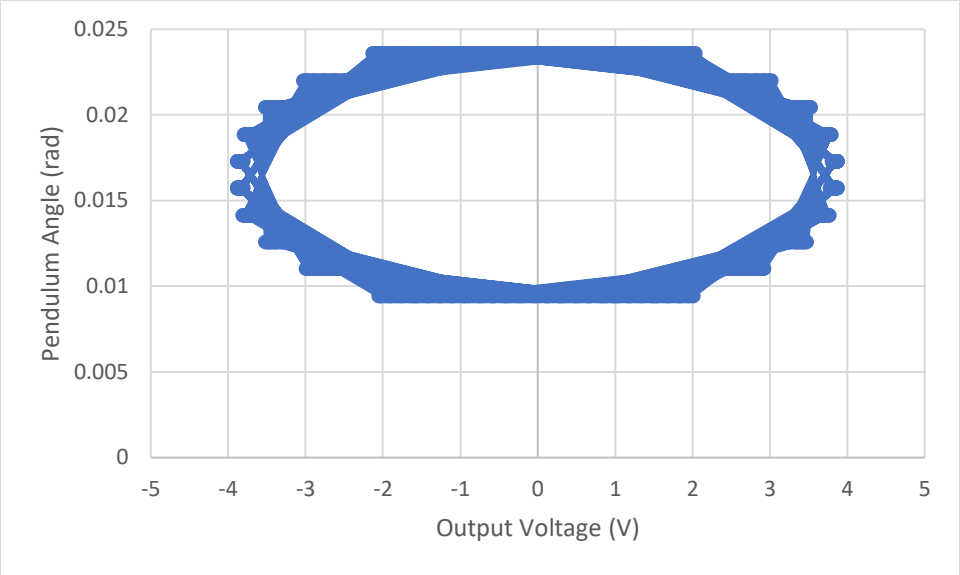


**Figure 7, Lissajous Plot at Resonance Frequency:** This is the Lissajous plot at the resonance frequency (0.657 ± 0.005) Hz. This major axis of this ellipse is horizontal, which indicates that it is at the resonance frequency. This plot was created with more than 500 data points so that the true shape of the graph could be seen.

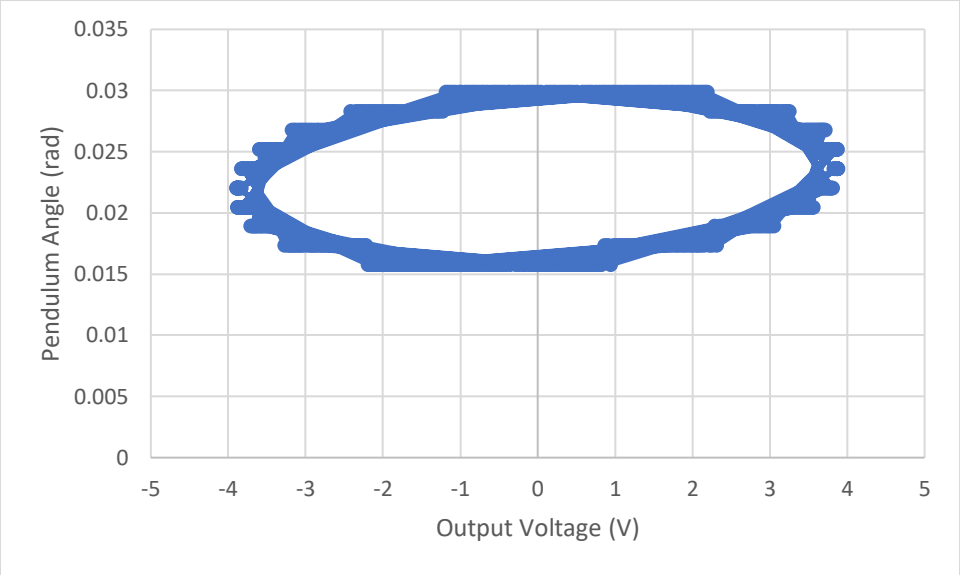


**Figure 8, Lissajous Plot Below Resonance Frequency:** This Lissajous plot was generated with a frequency (0.637 ± 0.005) Hz, which is below the resonance frequency. The major axis of the ellipse is tilted so that the right side is slightly higher than the left side.

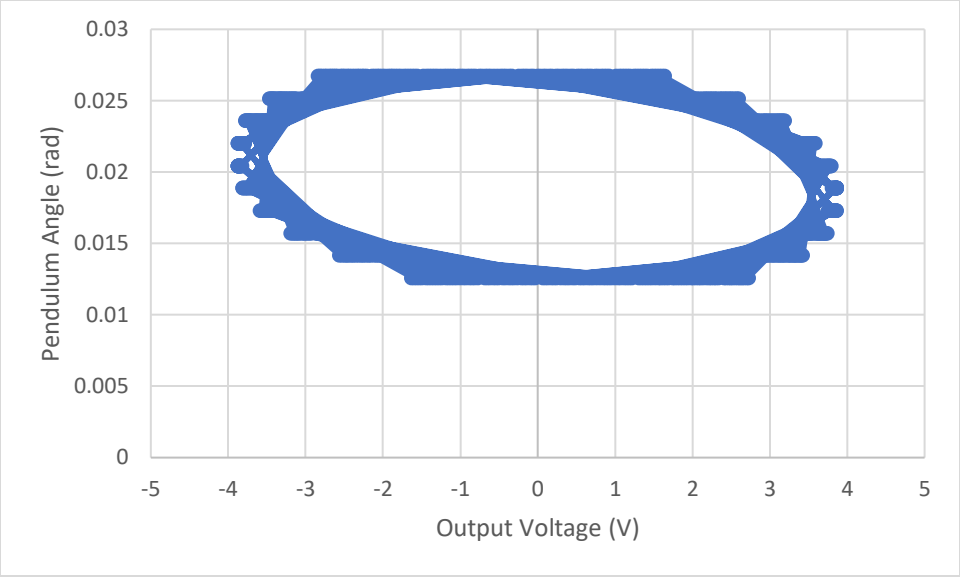


**Figure 9, Lissajous Plot Above Resonance Frequency:** This is Lissajous plot generated by using a frequency of (0.677 ± 0.005) Hz. This is above the resonance frequency of (0.657 ± 0.005). The major axis of the ellipse is tilted so that the left side is slightly higher than the right side.

For Figures 8 and 9, it would have been beneficial if we recorded data at frequencies that were further away from the resonance frequency to exaggerate the differences between the plots.

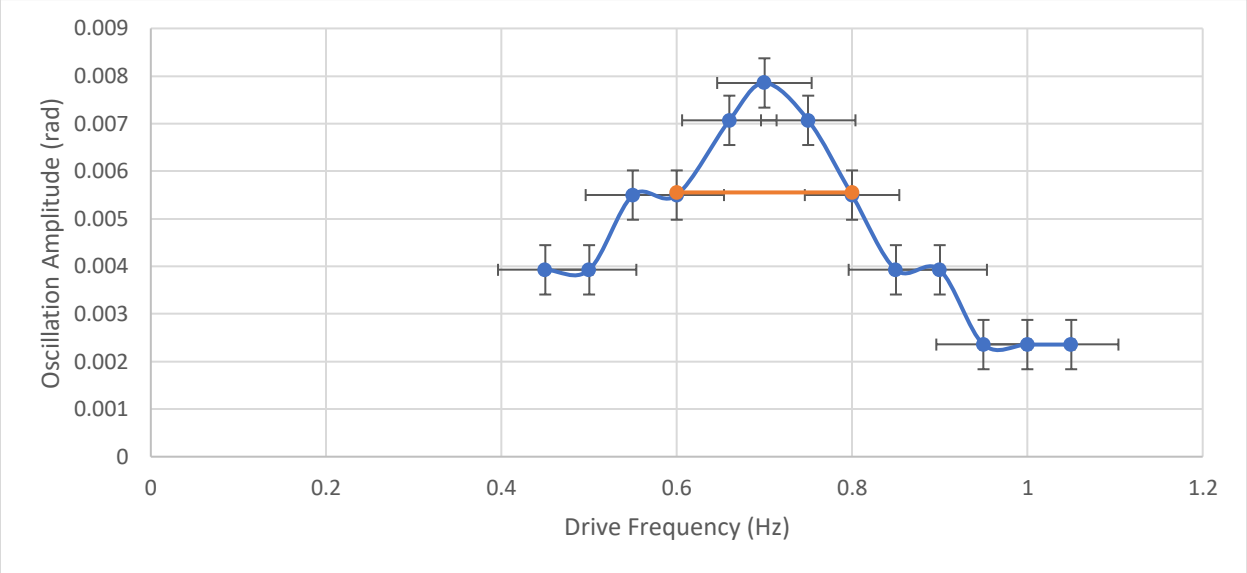


**Figure 10, Amplitude Response to Different Frequencies:** This plot shows the amplitude of oscillation at various frequencies. The orange line indicates the height which is $1/\sqrt{2}$ times the maximum amplitude of the graph. The resonance width is (0.20 ± 0.05) Hz. From the graph, the two values that intersect with the horizontal line are 0.60 Hz and 0.80 Hz.

We can see from this plot that the peak corresponds to the resonance frequency of (0.711 ± 0.001) Hz, which is what we expect. Our plot does not have a perfect Lorentzian shape because

some values were measured to be the same for different frequencies. However, if we had increased the precision of the measurement, we would likely have the correct shape.

*Q-Factor via Amplitude Response*

The two frequencies that we measured to have amplitude of $1/\sqrt{2}$ times the peak amplitude are 0.57 Hz and 0.8 Hz. The plot in Figure 10 nearly captures this, but we did not have the proper precision. These values provide us with a way to calculate the Q-factor with another method.

$$Q = \frac{\omega_0}{\Delta\omega} = 3.09$$

$$\partial Q = 0.22$$

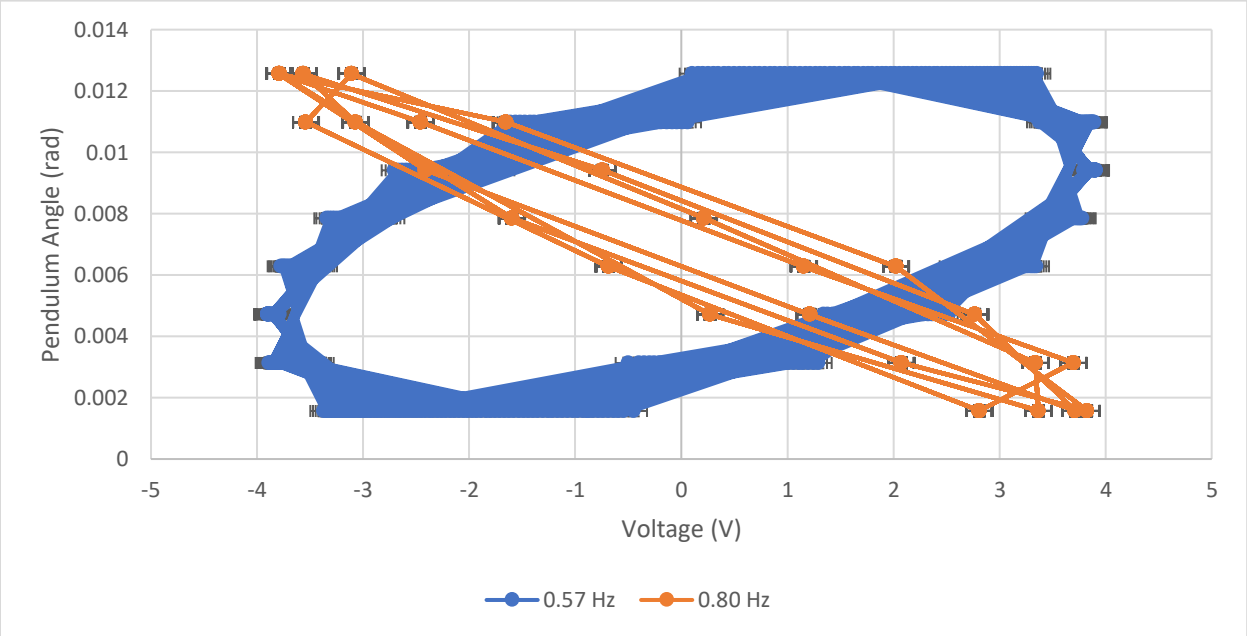


**Figure 11, Lissajous Plots for 0.57 and 0.80 Hz:** This plot shows the Lissajous plots of the two frequencies we measured an amplitude response $1/\sqrt{2}$ times the response generated by resonance frequency. Our Lissajous plot for 0.57 Hz produced a cleaner, more rounded graph than 0.80 Hz. We collected more than 500 data points for the trial using 0.80 Hz. The data points from each cycle were repeated from the last cycle. The graph overlaps and does not look as smooth as the plot for 0.57 Hz.

Our first and second method of determining the Q-factor produced nearly identical values. The first method yielded the Q-factor (1.71 ± 0.02) and the second method yielded a Q-factor of (1.71 ± 0.01). With the third method, our Q-factor was determined to be (3.09 ± 0.22).

All three methods have their own drawbacks. The first method involves doing more multiplications, which propagates uncertainty more than the second method. This yields an uncertainty for the first method that is higher than the uncertainty from the second method. The second method works well when Q >> 1.[1] Since we found that our Q-factor was relatively low, this indicates that the second method was not entirely reliable. The third method uses the amplitude width $\Delta\omega$. This method is imprecise because our amplitude response data was recorded with too low of a precision. Therefore, we had to estimate our value for the width $\Delta\omega$. This makes the calculation more inaccurate and yields higher uncertainty. Additionally, our graph showed that the horizontal line that was $1/\sqrt{2}$ the magnitude of our peak amplitude intersected our Lorentzian data plot in multiple places for the lower bound.

With high values of Q, the ratio of the driven, damped frequency to the undamped, undriven frequency should converge to one. Our value of $\omega_R$ = (0.657 ± 0.005) is 7.6% off from our undamped, undriven frequency. We expect the ratio $\omega_R/\omega_0$ to have a value of 0.924. If we plug in each Q-factor from each method into Equation 6.15, we can see which method returned the most accurate Q-factor.

When we plug in the Q-factors from method one and method two into the equation, we receive the value of 0.924, which aligns with the expected value of 0.924. The Q-factor of the third method returns a result of 0.975. Although we would like to see our results produce a higher Q-factor, the Q-factor from the third method does not accurately reflect the actual results of the experiment.

$$\frac{\omega_R}{\omega_0} = \frac{1}{\sqrt{1+\frac{1}{2Q^2}}} \quad (Eq.6.15)^1$$

The second method is the better method to use, even though it returned the same value as the first method. The second method yields a slightly lower uncertainty than the first method. The second method also uses only measured values whereas the first method requires more calculation, increasing the propagation of uncertainty to its results.

*Vibrating String*

The unstretched string has a length of (16.5 ± 0.4) cm and it has a mass of (15.1 ± 0.2) g. The unused length of string was (16.50 ± 0.05) cm. We need to subtract off this portion from the total unstretched length of the string. The string at the clamp and the loose end on the clamp side are one unstretched portion, and the string used in the knot at the hanging mass end is also unstretched. We find the ratio of the trimmed length to the total length and find that corresponding portion of the total mass of the spring. We find that the mass of the trimmed, stretched string is (12.4 ± 0.2) g. To find the linear density, we need to divide the mass of the stretch string by the length of the stretched string. We already have the stretched mass of the

string because this stays constant for each case. We need to find the length of the stretched string by subtracting each unstretched portion length from the stretched length in each trial.

$$\mu_{linear} = \frac{m_{stretch}}{L_{stretch}}$$

$$\partial\mu_{linear} = \mu_{linear\,best}\sqrt{\left(\frac{\partial m_{stretch}}{m_{stretch}}\right)^2 + \left(\frac{\partial L_{stretch}}{L_{stretch}}\right)^2}$$

| Trial | Mass (g) | Stretched String Length (m) | Applied Tension (N) | Linear Mass Density (kg/m) |
|---|---|---|---|---|
| 1 | 99.8 ± 0.2 | 0.228 ± 0.001 | 1.07 ± 0.05 | 0.00650 ± 0.00012 |
| 2 | 199.7 ± 0.3 | 0.230 ± 0.001 | 2.05 ± 0.05 | 0.00645 ± 0.00012 |
| 3 | 349.5 ± 0.5 | 0.234 ± 0.001 | 3.52 ± 0.05 | 0.00632 ± 0.00012 |

**Table 1, Length, Tension, and Linear Mass Densities by Attached Mass:** This table presents the string length, applied tension, and linear mass density of the system depending on the mass that was attached to the end of the string. Each segment of the string was measured separately to determine the full stretched length of the string. The applied tension was calculated by finding the total mass hanging off of the pulley (hanging mass and string mass) and multiplying by the gravitational constant 9.80 m/s$^2$.

Applied tension has units (kg*m/s$^2$) and linear mass density has units of (kg/m). We can attain the predicted wave speed if we divide the applied tension by the linear mass density and take the square root of the result.

$$v_{pred} = \sqrt{\frac{F_{tension}}{\mu_{linear}}}$$

To find the experimental wave speed, we can measure the distances between the peaks on the graphs which give us the time that the wave took to travel two lengths of the stretched string between the pulley and the clamp. The waves do not travel past the pulley when they are produced by the wave driver, so the pulley is where we end the measurement. We measure two lengths because the positive peaks in the graph are when the wave leaves the wave driver, and then comes back (it has traveled down the string and then back again).

$$v_{exp} = \frac{2L_{pulley\_to\_clamp}}{\Delta t}$$

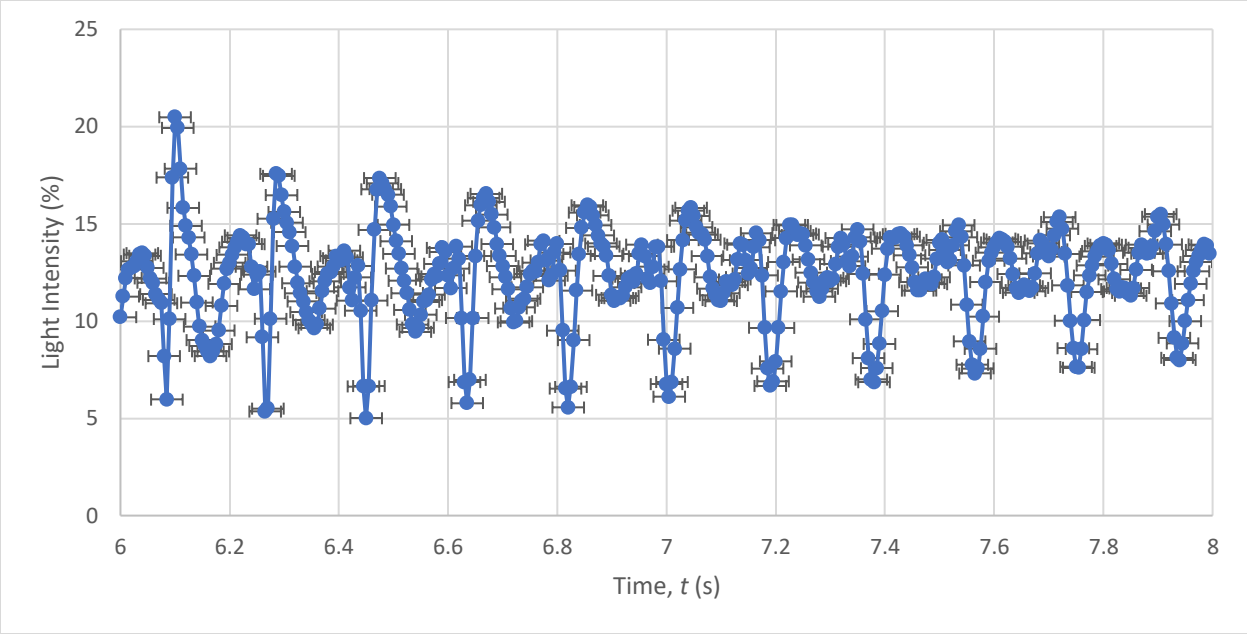


**Figure 12, String Oscillations with 100 g Attached:** This plot shows how the light intensity readings from the photodiode change as time goes on and the waves travel through the string. A 100 g mass was attached to the string in this trial to create tension on the string and allow the wave to travel through it. A wave was sent through the string every two seconds. The tallest peak in the graph on the left side represents where the pulse for this time span was generated. There is a decay in the amplitude of oscillation because the wave loses energy in the string due to environmental factors, such as sagging. The peaks that we measured to find the experimental wave speed are the top left of each 'M' shape.

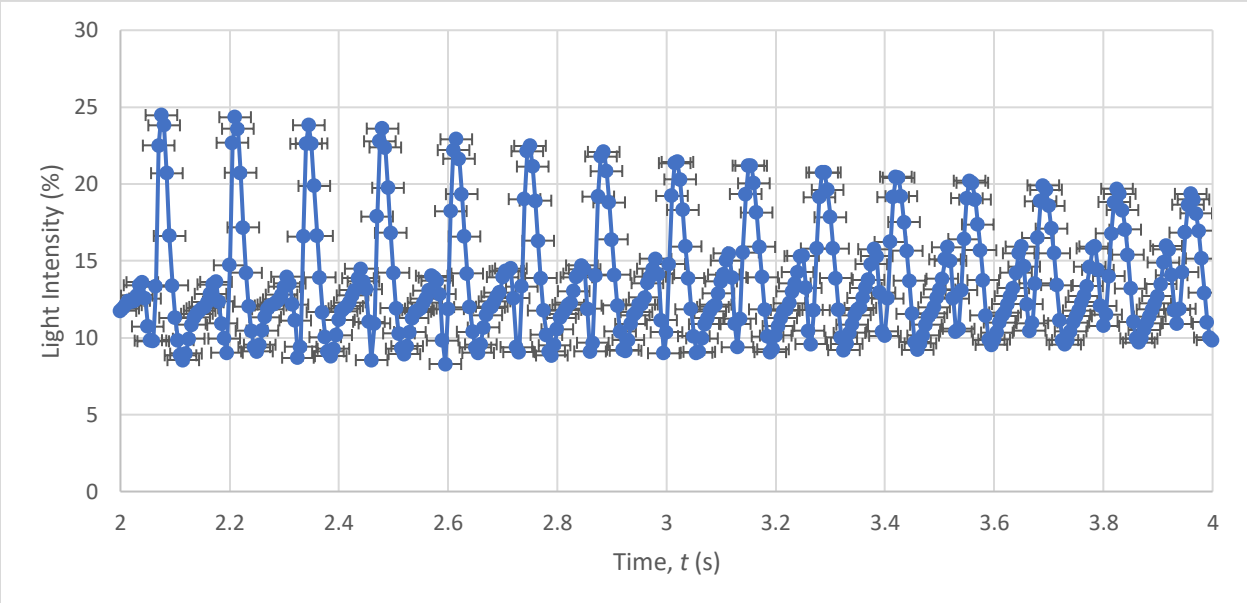


**Figure 13, String Oscillations with 200 g Attached:** This plot shows the change in light intensity recorded by the photodiode as the waves travel through the string with a 200 g mass attached. This plot is a bit cleaner than the plot in Figure 12 for the 100 g mass. We used each maximum

as the peaks to find the time differences for finding experimental wave speed. The leftmost peak is where the pulse was generated. As the wave loses energy, the amplitude of light intensity decays.

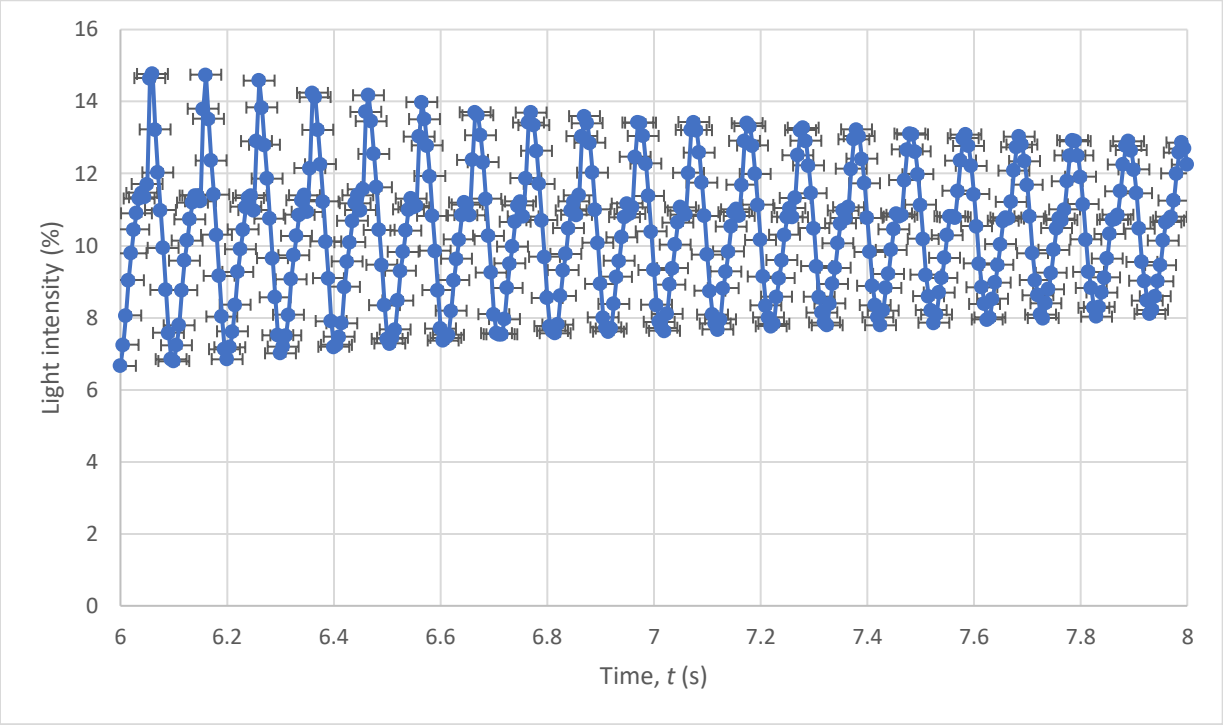


**Figure 14, String Oscillations with 350 g Attached:** This plot shows how the light intensity readings change as the wave travels through the string with a 350 g mass attached. There is a slight decay in the amplitude of the light intensity. This plot has less noise than the previous two.

There is a small horizontal offset along the x-axis of the peaks that represent when the pulse is generated because the photodiode is on the opposite side of the string from the wave driver. This is to say that the left most peak does not have an x-coordinate of 6 in Figure 12 and 14, and 2 in Figure 13. If we divide one length of the stretched string by the time between the offset in the x-axis to the first peak, we expect to see our calculated wave speed. For example, in Figure 14, the first peak comes at (6.055 ± 0.005) seconds. The left offset on the x-axis is 6, so we have (0.055 ± 0.005) seconds to travel (1.212 ± 0.006) meters. If we divide the distance by the time, we get the result of (22.04 ± 0.01) m/s, which is close to our experimental wave speed of (24.05 ± 0.04) m/s (from Table 2 below) for this trial.

There is less noise in the oscillations for when the 350 g was attached to the string. We noticed that there was some sag in the string for the two smaller masses. This is might be the reason for the extra noise in the oscillations when 100 g and 200 g were attached.

| Mass (g) | Predicted Wave Speed (m/s) | Experimental Wave Speed (m/s) |
|---|---|---|
| 99.8 ± 0.2 | 12.8 ± 0.6 | 12.83 ± 0.07 |
| 199.7 ± 0.3 | 17.8 ± 0.5 | 17.96 ± 0.01 |
| 349.5 ± 0.5 | 23.6 ± 0.6 | 24.05 ± 0.04 |

**Table 2, Wave Speeds in the String:** This table shows the predicted and experimental wave speed in the system depending on the mass that was attached to the end of the string. The predicted wave speed was calculated taking the square root of the value of applied tension divided by the linear mass density of the string. The experimental wave speed was found by finding the time it took the wave to travel down the length of the string and back. We divided twice the length of the string by this value of time.

As we would expect, our values agree in both cases. Each pair of corresponding wave speeds fall within each other's error windows. The corresponding values of the first two pairs values are less than 1% different from each other and the third pair's values are less than 2% different from each other. Propagation of uncertainty caused the predicted wave speed to have a much higher value of uncertainty. We were very deliberate in making our length measurements accurate, which likely helped the two wave speeds line up properly.

We can find the expected frequency of each harmonic using equation 7.3 from the lab manual[1]. We kept the (349.5 ± 0.5) g mass attached to the string during these trials, so we use the experimental wave speed for that mass. Our stretched length of string is (1.212 ± 0.006) m.

$$f(n) = \frac{nv}{2L_{pulley\_to\_clamp}}$$

$$\partial f_{best}(n) = f_{best}(n)\sqrt{\left(\frac{\partial v_{best}}{v_{best}}\right)^2 + \left(\frac{\partial L_{best}}{L_{best}}\right)^2}$$

The measured frequencies for each harmonic were determined by finding the frequencies at which the Lissajous plots generated by the DAQ were horizontal and symmetric across the y-axis. For each harmonic, we used the predicted frequency as a starting point and increased or decreased the frequency to find the correct one.

| $n^{th}$ harmonic | Predicted Frequency (Hz) | Measured Frequency (Hz) |
|---|---|---|
| 1 | 9.92 ± 0.05 | 9.81 ± 0.03 |
| 2 | 19.84 ± 0.10 | 19.3 ± 0.1 |
| 3 | 29.76 ± 0.16 | 28.6± 0.1 |
| 4 | 39.69 ± 0.21 | 40.2 ± 0.2 |
| 5 | 49.61 ± 0.26 | 49.0 ± 0.04 |
| 6 | 59.53 ± 0.31 | 60.5 ± 0.6 |
| 7 | 69.45 ± 0.36 | 71.2 ± 0.6 |
| 8 | 79.37 ± 0.41 | 79.7 ± 0.8 |
| 9 | 89.29 ± 0.47 | 91 ± 1 |

**Table 3, Frequencies for Each Harmonic:** This table shows the predicted and measured frequencies for each harmonic for our string. The predicted frequencies were generated by using equation 7.3 from the lab manual[1], and the measured frequencies were determined by looking at the Lissajous plots from the DAQ. The uncertainty increases as the measured frequencies because we began to run out of time. Thus, we were unable to narrow down the range of values for measured frequency as much as we would have liked to.

Our values tend to agree here as well, although some pairs of predicted and measured frequency fall out of each other's error windows. Each pair's corresponding values are within 4% or less of each other. As we moved to higher harmonics, it became increasingly difficult to discern the nodes from the antinodes. It was clear at the lower harmonics because the amplitudes of the antinodes were much greater than the antinodes at higher harmonics. We looked at the $30^{th}$ harmonic after predicting the harmonic frequency to be around (292 ± 2) Hz. However, we were not able to tell the nodes apart from the antinodes. The entire string seemed to be vibrating, but we know that this is not really the case. Since it was vibrating at the $30^{th}$ harmonic, there must be 30 nodes in the vibrating string.

Next, we look at the second, fourth, and fifth harmonic while the string is constrained in the middle and when it is unrestrained. We aim to see whether each harmonic's restrained and unrestrained plots resemble each other.

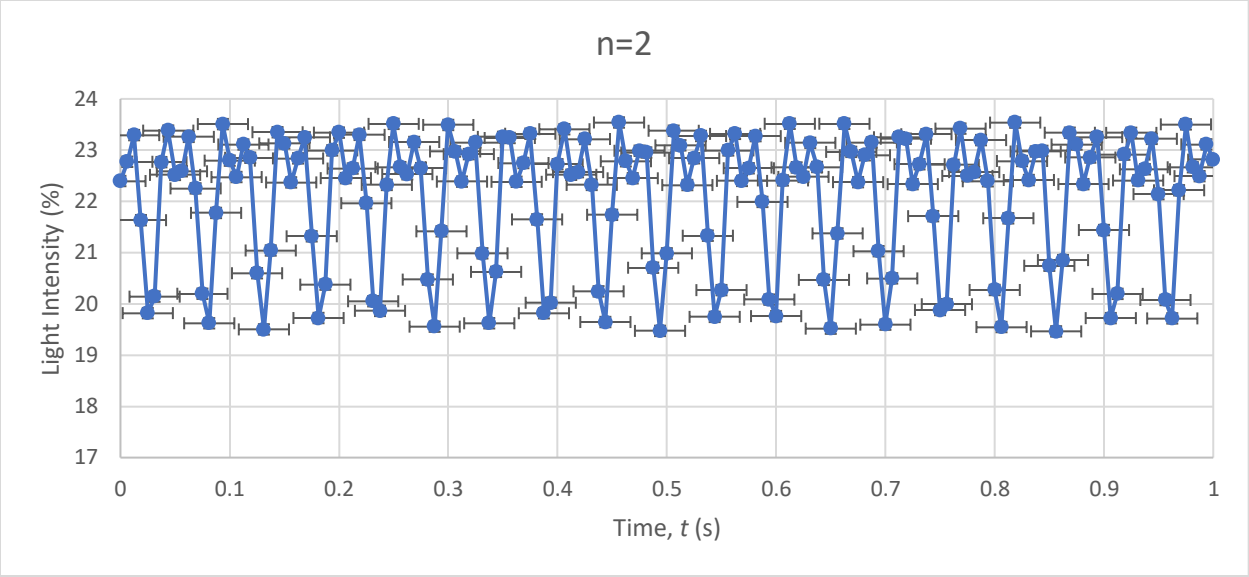


**Figure 15, Second Harmonic Restricted Oscillations:** This plot shows the oscillations of the stretched string in the second harmonic. The string is pinched with two fingers in the middle of the string. Since the second harmonic is an even harmonic, there is a node where we pinched the string. This allowed to plot to resemble the plot of an unrestricted oscillation plot of the same harmonic. However, since we ran out of time to record the unrestricted oscillation data, that plot is not shown. The maxima and minima are fairly consistent throughout the data set. This indicates that we pinched the string in the correct place on the string (almost exactly at the node).

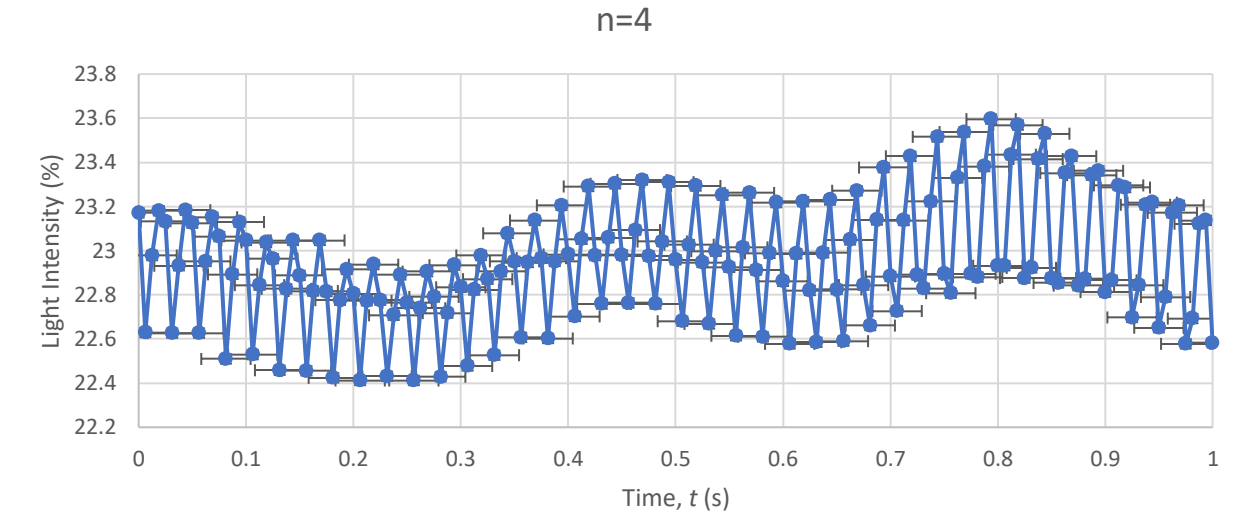


**Figure 16, Fourth Harmonic Restricted Oscillations:** This is the plot of the string's oscillations at the fourth harmonic. This is also an even harmonic, so the plot likely resembles the unrestricted oscillation plot. We pinched the string in the middle, and the fourth harmonic has a node in the middle. The shift of the graph up and down was likely because we pinched the string with our fingers. The shakiness of our hands would have shifted the string up or down, which could cause the light sensor to have varying readings.

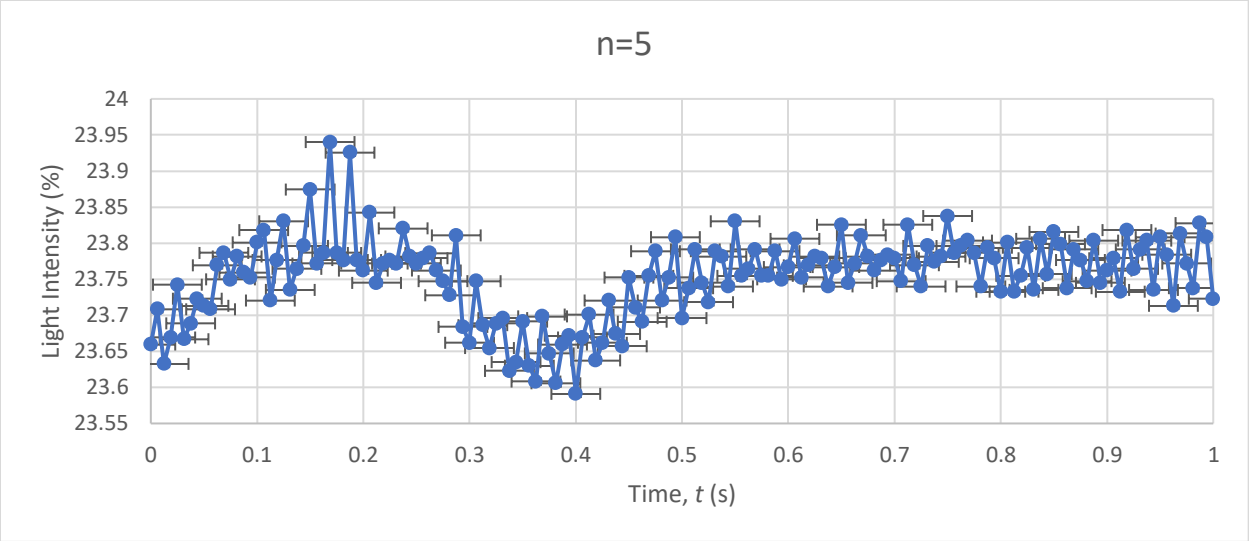


**Figure 17, Fifth Harmonic Restricted Oscillations:** This plot shows the oscillation of the string at the fifth harmonic while pinched in the middle. It likely does not resemble the plot for the unrestricted oscillation because the string is pinched in a place where the string has an antinode at the fifth harmonic. This restricts the antinode from having its full amplitude of oscillation and disturbs the harmonic oscillation.

Unfortunately, we ran out of time while conducting the experiment, so we were only able to attain data for the constrained cases. Our plots may have a slightly reduced amplitude because we used our fingers to pinch the string instead of a ring. However, we would expect the plots of the graphs for the n=2 and n=4 harmonic to generally resemble the plots of restricted oscillation. This is because these two harmonics have a node where the string is pinched. However, the unrestricted n=5 harmonic plot will not look like the restricted plot because the string is pinched at an antinode. We can extrapolate our findings and say that the restricted oscillation plots of even harmonics will look like their unrestricted counterparts. In contrast, plots of restricted oscillations for odd harmonics will not look like the unrestricted oscillation plots. The restriction needs to be at a node for the plot of the restricted oscillation to look like the plot of the unrestricted oscillation.

**Conclusion**

In the physical pendulum experiment, we look at the three damping regimes, the resonance frequencies for damped and undamped oscillations, and the Q-factors of the oscillator systems.

For the undamped, we measured a resonance frequency of (0.711 ± 0.001) Hz. We determined this result by looking at the number of oscillation cycles were completed within a certain time span. The resonance frequency in the damped, driven trial was determined by looking at the Lissajous plots of different frequencies. We looked for which value produced an ellipse with a horizontal major axis. We expected to find that the resonance frequencies for the damped and undamped trials would be the same. However, we measured a resonance frequency of (0.657 ± 0.05) Hz in the damped trial.

We calculated the Q-factor of the oscillator with three different methods. The first and second method produced values of (1.71 ± 0.01) Hz and (1.71 ± 0.02) Hz respectively. These results agree with the expected Q-factor considering the difference between our resonance frequency in the drive, damped oscillations and undriven, undamped oscillations. The third method produced a higher Q-factor of (3.09 ± 0.22). This value did not accurately represent the relationship between the two resonance frequencies. Because of the minimal propagation of uncertainty, it was determined that the second method was the most accurate among the three methods used to find the Q-factor.

This discrepancy between our resonance frequencies for each trail could have been caused by several factors. It is possible that the rotation sensor introduced friction that affected the undamped trial more than the damped trial, or vice versa. The oscillation in the undamped trial had a higher amplitude of angular displacement than in the damped trial. Depending on which parts of the rotation sensor had the most friction, one trial may have been affected while the other one was not. Additionally, it was difficult to hold the pendulum at the correct depth during each release. After releasing the pendulum, it would shake back and force along the axis of torque (z-axis) of the system.

To prevent these discrepancies, we could use the same angular displacement amplitude for both trials. This way, the friction would affect both trials the same. Additionally, we could use a release mechanism to prevent the shaking of the pendulum. The releases would be consistent and smooth for each release. Also, we should increase the precision of our measurements to improve our plot of amplitude response. With higher precision, we would likely get the Lorentzian shape that we are looking for in Figure 10.

For the vibrating string, we investigated the wave speed and harmonics of the system. We began by finding the applied tension in the string as well as the linear mass density. As we increased the mass that was attached to the hanging end of the string, the applied tension increased, and the linear mass density decreased. The tension increased as mass increased because there was a higher gravitational force pulling the mass downward, which was translated into string tension via the pulley. The linear mass density decreased because the same amount of mass in the stretched string is spread across a longer length as the string is pulled down by the mass.

With the applied tension and the linear mass density, we were able to calculate predicted values for the wave speed through the string for each mass that was hung. For our experimental values of wave speed, we looked at the time that it took the wave to travel from the wave driver to the pulley and back to the wave driver. We divide the distance covered by the wave (equivalent to two lengths) by the time it took to travel from one end of the string to the other and back again. The calculations for the predicted wave speed and the experimental wave speed both return values with units of meters per second, which is what we expect. Our experimental values were all within 2% of their predicted wave speed counterparts. This demonstrates that the two methods of calculating the wave speed are equivalent.

Next, we looked at the frequencies of the wave driver pulses to produce each *n*-harmonic of the string. Again, we first produced our predicted frequencies using equation 7.3 from the lab manual.[1] We used these predictions as a starting point when looking for the actual frequencies. We used the DAQ interface to produce pulses with the wave driver at frequencies that we specified. We looked at the Lissajous plots which plot light intensity against output voltage. When the plots are horizontal and symmetric across the y-axis, this means that the frequency that was used to produce them is the frequency of a harmonic. Using this method, we found the frequencies of the first through ninth harmonic. For these values, our experimental values were within 4% of their corresponding predicted values. Therefore, we verified that those two methods also produce equivalent values.

Finally, we investigated the effect of pinching the string halfway between the pulley and the wave driver. We pinched the string with our fingers because we did not have time to set up the proper apparatus. We used the DAQ to produce waves with the wave driver at the second, fourth, and fifth harmonic frequency. We hypothesize that for the second and fourth harmonic frequencies, the plots of the light intensity over time would resemble the plots of the same harmonic oscillation without a restriction. We further extrapolated that this trend is true for all even harmonics. Though we do not have the data to confirm this hypothesis, it makes sense because even harmonics have a node at the middle point, so pinching the string where it does not oscillate should have a minimal effect on the harmonic oscillation. However, for the fifth harmonic, the shape of the graph did not look uniform as a harmonic oscillation plot should. We also hypothesize that odd harmonics have a significant effect on the oscillation. The restriction is at a point on the string where odd harmonics have an antinode. This disrupts the harmonic oscillation, so we should see results consistent with oscillation at the odd harmonics

While collecting data, several factors may have introduced error into our experiment. First, there was noise in the plots of the oscillation when the 100 g and 200 g masses were attached to the string (Figure 12 and 13). In the 350 g trial, we notice that there is less noise. The string sagged more in the 100 g and 200 g trials, so it is possible that this introduced the extra noise. The sag also explains why the amplitude of the wave decreased more rapidly in the first two trials, but less rapidly in the third trial. Also, the amplitudes of oscillation were likely reduced in the third part of this experiment because we used fingers to pinch the string. Sometimes the string would even slip out from in between the two fingers because the vibrations made it difficult to keep it in place. In addition, some of the data we recorded was not as precise as we would have liked it to be, especially in the second and third parts of the experiment. We had to make rough estimates for some of the frequency ranges for each harmonic. We did not have enough time to narrow it down, and Table 3 reflects this with increasing uncertainties for each successive harmonic.

The main way to improve this experiment is to work more efficiently. This way we can record all the data needed, and we can also get more precise measurements. One improvement we can make is to have all pieces of our equipment set up before collecting data. This would allow us to keep recording data without having to stop and assemble the next piece of the apparatus. We

also need a way to make our measurements more accurate. We occasionally had to hold the ruler in the air to take measurements. Physically, we cannot keep our arms completely still, so there was a significant amount of uncertainty when taking these measurements. Instead of a meter ruler, a tape measure would be far more useful and practical. We should also make our equipment more stable to begin with. That way, we do not need to use counterbalances (Figure 3) to keep our equipment from falling. There were a few times in which we had to re-setup our equipment, which introduces more error and inconsistency into the experiment.

**Bibliography**


1. Campbell, W. C. et al. Physics 4AL: Mechanics Lab Manual (ver. June 27, 2018). (Univ. California Los Angeles, Los Angeles, California).